

Notes on optical fibres and fibre bundles

Introduction

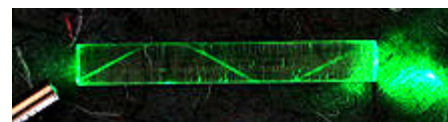
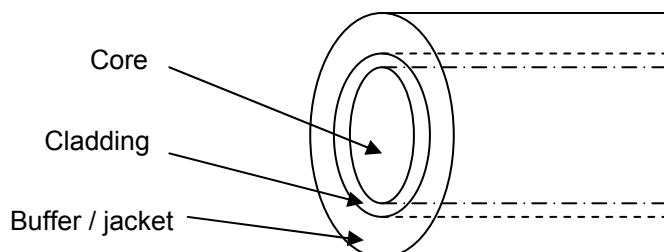
This note has been prepared with the intention of putting of summarising salient facts about optical fibres. Of course the selection of the characteristics presented is inevitably limited and biased. Limited since there are numerous textbooks and websites which are available for more detailed explanations and biased as the intention was to present details which are more important for work in the biosciences rather than in telecommunication applications. It is hoped that the students who are not too familiar with optics will find this note useful and that the interested reader will be spurred on to search elsewhere for further details.

The technology of fibre optics, is a relatively simple and old technology. Guiding of light by refraction, the principle that makes fibre optics possible, was first demonstrated in the early 1840s by D Colladon and J Babinet in Paris. Practical applications, such as close internal illumination during dentistry, appeared early in the 20th century. The principle of using optical fibres for image transmission was first used for internal medical examinations by H Lamm in the 1930s. Modern optical fibres have a transparent cladding around the core to enhance light guidance. Developments on fibre bundles for image transmission were pioneered by H Hopkins and NS Kapany at Imperial College in London in 1954: they achieved low-loss light transmission through a 75 cm long bundle using several thousand fibres. The first fibreoptic semi-flexible gastroscope was patented by B Hirschowitz, CW Peters, and LE Curtiss, researchers at the University of Michigan, in 1956. In the process of developing the gastroscope, Curtiss produced the first glass-clad fibres; previous optical fibres had relied on air or impractical oils and waxes as the low-index cladding material.

J Nishizawa, proposed the use of optical fibres for communications in 1963. He also invented other technologies that contributed to the development of optical fibre communications, such as the graded-index optical fibre. The first working fibre-optical data transmission system was demonstrated by at Telefunken Research Labs in Ulm in 1965. CK Kao and GA Hockham from the company Standard Telephones and Cables (STC) were the first to promote the idea that the attenuation in optical fibres could be reduced below 20 dB/km, making them a practical communication medium. They correctly suggested that attenuation is caused by impurities that could be removed, rather than by fundamental physical effects such as scattering. They correctly and systematically theorized the light-loss properties, and suggested the use of high purity silica glass.

Optical fibres

Optical fibres, lightpipes, and light guides are essentially similar and operate on similar principles. They each contain a central transparent core, usually circular in cross-section, surrounded by an annular cladding. This cladding has a lower refractive index than the core. In some cases, the cladding can be air. The details of an optical fibre are shown in the figure below. A large-scale simulation is also shown above



The core can transmit light for long distances with low loss because total internal reflection takes place at the interface between the core and the cladding. The primary purpose of the cladding is to maintain the integrity of this interface. Without it, total internal reflection will occur at the core-air interface, but surface contaminations such as dust, nicks etc. reduce the transmission to unacceptably low levels. Often layers of buffering and/or jacketing are placed

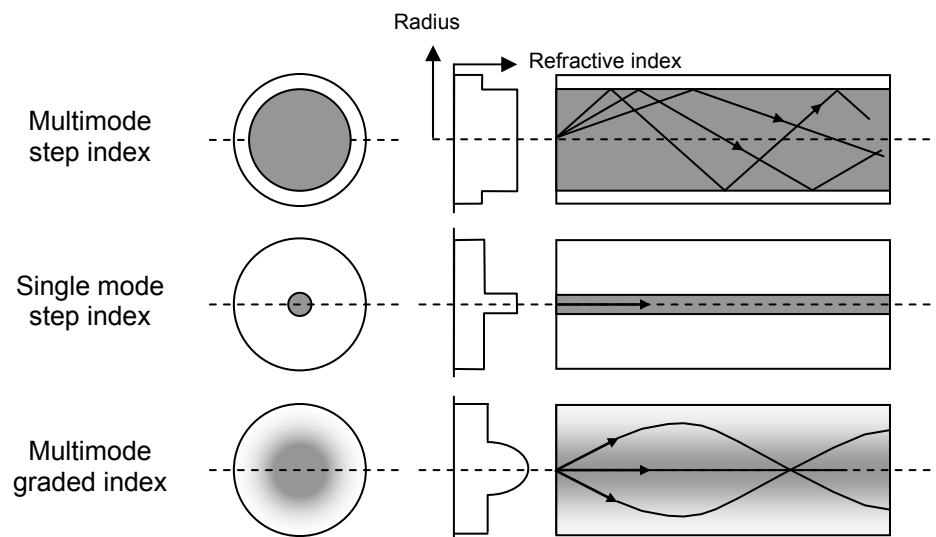
outside the cladding and provide additional protection, particularly when the core and or cladding are made of glass.

The core diameter can range from very small, on the order of the wavelength of light, to a several millimetres or more. The very thin cores are essentially waveguides and not used for illumination, but rather for signal transmission. Flexible glass and silica (quartz) fibres have core diameters which range from $\sim 50 \mu\text{m}$ to about $1000 \mu\text{m}$. The material is usually glass, quartz or plastic. For special applications, other exotic materials such as liquid light guides, sapphire, fluoride or calcogenide additives (mainly sulphur-based such as As-S or Ge-S) may be used. There are some unavoidable requirements for good light transmission, such as pure glass materials for the core and cladding and high transparency in the part of the optical spectrum used. Minimal optical dispersion is also necessary. The economics and quality of the fibre are dictated by a number of process parameters such as glass transformation temperature, viscosity, inclusions and chemical affinity. Light launched into a fibre will, after a given length, reach the core material boundary and pass to another medium (glass, air, etc.). Depending on the incident angle, some of the energy will be refracted outward (leaky modes) and some will reflect back into the core material (guided modes).

If they are much thicker than $\sim 1 \text{ mm}$, the fibres become rigid and are then called rods or light pipes. Plastic fibres are flexible at thicker core diameters. It is also possible to use liquid cores and plastic cladding in order to make flexible, high-transmittance light guides. These can have core diameters of 10 mm or more. Fibres that support many propagation paths or transverse modes are called multi-mode fibres, while those that only support a single mode are called single-mode fibres. Multi-mode fibres generally have a wider core diameter, and are used for short-distance communication links and for applications where high power must be transmitted. Single-mode fibres are used for most communication links longer than $\sim 1 \text{ km}$.

Graded-index or gradient-index fibres have cores constructed such that the refractive index decreases with increasing radial distance from the fibre axis (an imaginary central axis running down the length of the fibre). Because parts of the core closer to the axis have a higher refractive index than the parts near the cladding, light follows sinusoidal paths down the fibre. The most common refractive index profile for a graded-index fibre is near to being parabolic. Such a profile results in continual refocusing of the light in the core.

These are illustrated below:



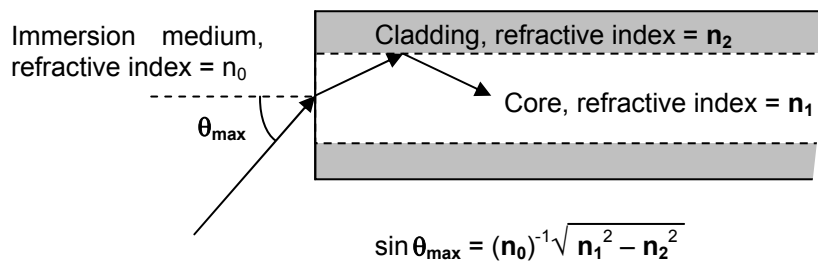
In the early 1990s the first photonic-crystal fibres were developed. These devices guides light by exploiting diffraction effects from a periodic structure, rather than by total internal reflection to confine light to the fibres core. Photonic crystal fibres are able to transport much higher powers than conventional fibres. In addition their properties can be made wavelength-dependent to improve performance. Photonic-crystal fibres are made with a regular pattern of

index variation, often in the form of cylindrical holes that run along the length of the fibre (Holey fibres).

Some special-purpose optical fibres are constructed with a non-cylindrical core and/or cladding layer, usually with an elliptical or rectangular cross-section. These include polarization-maintaining fibres and fibres designed to suppress whispering gallery mode propagation. Polarization-maintaining fibres are unique type of fibres and are commonly used in fibre optic sensors where a physical process is arranged to change the polarisation and hence develop and intensity change in the output of the fibre.

Numerical Aperture and Étendue

The maximum angle that a fibre can accept and transmit depends on the refractive indices of the core and cladding (as well as the refractive index of the surrounding medium, usually air, $n_0 = 1$).



and the numerical aperture is: $NA = n_0 \sin \theta_{\max} = \sqrt{n_1^2 - n_2^2}$

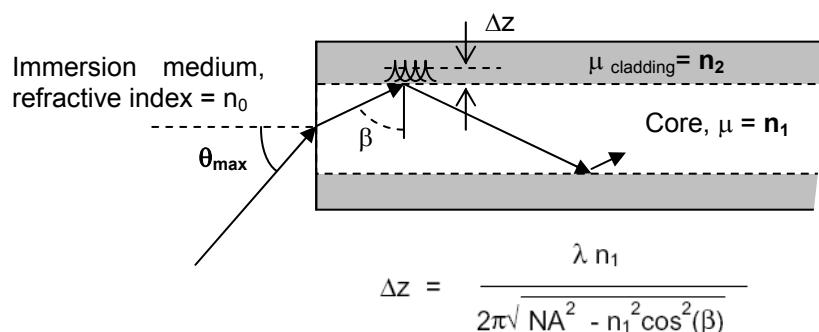
The fibre has a maximum acceptance projected solid angle, $\Omega = \pi \sin^2 \theta_{\max}$, and an acceptance area equal to the cross-sectional area of the core. Together, they define the throughput or étendue for the fibre in air:

Étendue = $(\pi^2/4)d^2 NA^2$ where **d** is the core diameter.

This étendue defines the ability of the fibre to transport light flux when it is irradiated by an appropriate light source. A fibre illuminated at less than its maximum acceptance angle will, theoretically, preserve the illumination angle at its output. However, bending and scattering at the core-cladding interface broadens this angle toward the maximum allowable. This effect is not important in illumination systems in which it is desirable to utilize the maximum étendue and fill the full input numerical aperture.

Guided light outside the core

When internal reflection takes place, a portion of the energy in the electric field penetrates the cladding. This gives rise to what is termed an 'evanescent field', as shown below. The penetration depth is typically ~5 times the wavelength of the light entering the fibre.



To simplify matters, subsequent mathematical descriptions of light transmission in the fibre are treated as planar waveguide-configurations. For such a planar light guide, the penetration depth of a transverse electromagnetic wave in the medium n_2 is given by:

$$\Delta z = \frac{\lambda n_1}{2\pi \sqrt{NA^2 - n_1^2 \cos^2(\beta)}}$$

Should β reach the critical angle for total internal reflection (1), the penetration depth Δz becomes ∞ . If $\beta = 90^\circ$, then $\Delta z = \lambda n_1 / (2\pi NA)$

The fact that a portion of the energy is transmitted in the cladding places constraints on the type of material used for the cladding. Further, it should be noted that the reflected wave experiences a phase shift dependent on β .

The phase shift, immediately after the reflection, causes the sine wave of the spreading ray to wander with the same periodicity (frequency). The phase shift, $\Delta\phi(\beta)$, repeats every 2π .

$$\Delta\Phi(\beta) = -2 \arctan \left[\frac{\sqrt{\sin^2(\beta) - (n_2/n_1)^2}}{\cos(\beta)} \right]$$

For the sake of completeness, it should be stated that transversal magnetic wave modes (TM) exist orthogonal to the electric wave modes (TE). Hence, for a mode number n there are two propagation wave modes (TE_n and TM_n). Equivalent relationship exists for Δz and $\Delta\phi(\beta)$ modified for TM wave modes.

Light absorption in fibres

Absorption losses are largely due to impurities in glass material from residual often unwanted atoms and hydrogen/oxygen molecules. Lastly, there are attenuation maxima in small band wavelength regions. The fundamental attenuated wavelength (highest absorption) is due to OH^- ions. In quartz this absorption is at $\lambda = 2.7 \mu m$. In the spectral region below this wavelength, there are other absorption bands at $1.38 \mu m$, $1.24 \mu m$, 950 nm and 720 nm . Between these wavelength bands windows of minimal attenuation exist. These spectral regions are at 850 nm , 1300 nm and at 1550 nm . These regions are used for data transmission. Unwanted impurities include metal ions such as Cr^{3+} , Fe^{2+} and Cu^{2+} , absorbing between 500 nm and 1000 nm .

When transmitting short wavelengths (UV light $\lambda < 250 \text{ nm}$) in quartz a damage mechanism referred to as solarisation occurs. In the quartz structure, there are absorption centres where negatively charged ions are replaced by electrons. Such regions in the crystal are also called colour centers, because the normally colour neutral crystals (e.g. NaCl) become characteristically discoloured.

In addition to absorption, scattering can also take place. One significant scattering mechanism at low wavelengths is Rayleigh scattering. Spatially there are high density gradients which alter refraction index and thereby cause scattering. The intensity of the scattered light is proportional to λ^{-4} . The effect evidences itself in, among other things, strong reverse scattering.

Another scattering mechanism is Mie scattering, which mainly results in forward scattering. This mechanism comes from material inhomogeneities at longer wavelengths. Finally, Stimulated Raman Scattering and Stimulated Brillouin Scattering are non-linear radiation induced effects, which take place when particular intensity thresholds are exceeded. In practice, such non-linear effects only take place when high intensity laser light is transmitted.

Losses due to fibre bending

Fibre bending produces at least two loss mechanisms:

a) In multimode fibers, the number of propagating modes is reduced as a function of the fibre bend radius according to:

$$M(R) \approx M_0 (1 - D_F n_2^2 / (R NA^2))$$

where M_0 = number of propagating modes when no bending is present

$M(R)$ = number of propagating modes when bending is present

n_2 = refractive index of cladding

R = bend radius

D_F = fiber diameter

NA = fibre numerical aperture

The percentage of light leaking from the different modes is:

$$\Delta M/M \approx 100 \times D_F n_2^2 / (R NA^2) \%$$

From the equation above it can be seen that fibres with small diameters and high numerical apertures should be used when such losses are to be minimised.

b) An additional problem when fibres are bent is electromagnetic radiation loss due to differences in propagation (wave front) velocity. The principal portion of electromagnetic energy is concentrated in the fibre core, while other portions are transmitted in the cladding and a slight amount outside the cladding.

When bending the fibre with bending radius R , the light will propagate with the medium's propagation velocity. In the fibre cross section, the area radially further from the radius centre will need to move with a greater velocity than that of the fibre core in order to maintain the signal transport speed. When a critical value is reached, z_{kr} , a limit is reached. The speed of light in a medium can not exceed its natural value $c = c_0/n_1$ (with $c_0 = 2.9979 \times 10^8$ m/s and n_1 = index of refraction of the core).

The transport velocity is then beyond this value. Since the signal velocity no longer exists, light can no longer be transmitted in this configuration and a portion of the energy radiates into the surroundings.

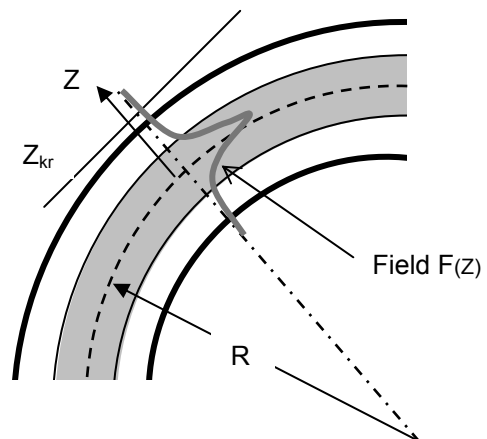
These effects are illustrated on the right.

All these losses contribute to increased attenuation. For multimode fibres, this effect is relatively small when compared to the reduction of propagating modes. However, this type of attenuation can seriously affect single mode fibres when they are bent.

For single mode fibres the attenuation coefficient is calculated from:

$$\alpha_B = (c/\sqrt{R}) e^{-pR}$$

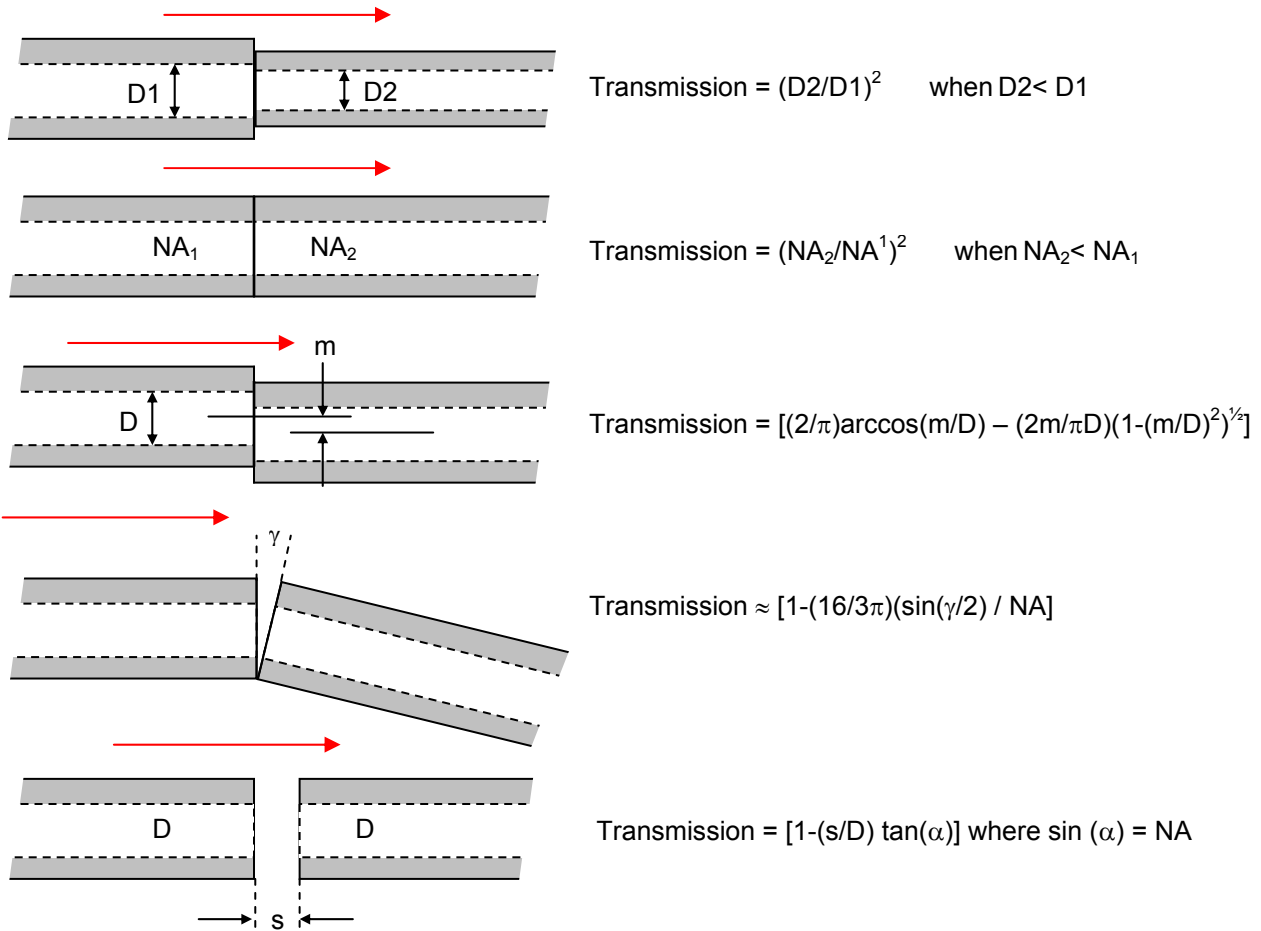
Where c and p are constants depending on fibre manufacture and wavelength. The stronger the electromagnetic field of transmitted modes out of the core, the more pronounced this effect. The field on the far side of the centre bend radius reaches the speed of light at distance z_{kr} , leading to light radiation outside the fibre. As wavelength increases, this effect needs to be taken progressively into account.



Losses associated with two coupled fibres

When two fibres are coupled, additional losses occur. These losses depend on the type(s) of fibre, the extent of separation and on degree to which the fibres are aligned. In practice, such coupling losses can be minimised through the use of refractive index matching or coupling gel, the use of ball lenses between fibres or more elaborate optical systems. Each of these inevitably adds different types of loss however.

Some of the consequences of coupling fibres are outlined below.



Transit time through fibres

When short light pulses are coupled into a fibre, the time behaviour is strongly influenced by the fibre type and by the core and cladding materials. Transit time differences lead to a of bandwidth limitation. These time differences are due to dispersion. There are two basic types of dispersion: (a) mode dispersion and (b) chromatic dispersion due to light dispersion in the material and due to light propagation in the fibre.

Mode dispersion results from differing transit times for different modes, in turn resulting from differing optical paths. This is obviously only true for multimode fibres. Single mode fibres only allow a single mode to propagate and thus no transit time effects are associated with such fibres. Graded index fibres theoretically have the same optical path for all modes. Light rays travel faster the closer they are to the interface due to the decreasing refractive index when moving from the core to the cladding interface and thus different modes travel in different spiral paths. Lower modes travel through a shorter path, as they propagate nearer the optical axis, but are also in a material of larger refractive index. Higher modes travel through a longer path length, but travel in a material of lower refractive index. The 'path length and index of refraction' product is constant and any transit time differences are therefore minimised.

The refractive indices of the core and cladding are wavelength dependent. Differing wavelengths travelling in the same medium are thus affected by differing refractive indices. As the velocity at a given wavelength λ in any medium is given by:

$$v(\lambda) = c/n(\lambda) \text{ where } c = \text{speed of light in vacuum and } n = \text{refractive index of medium,}$$

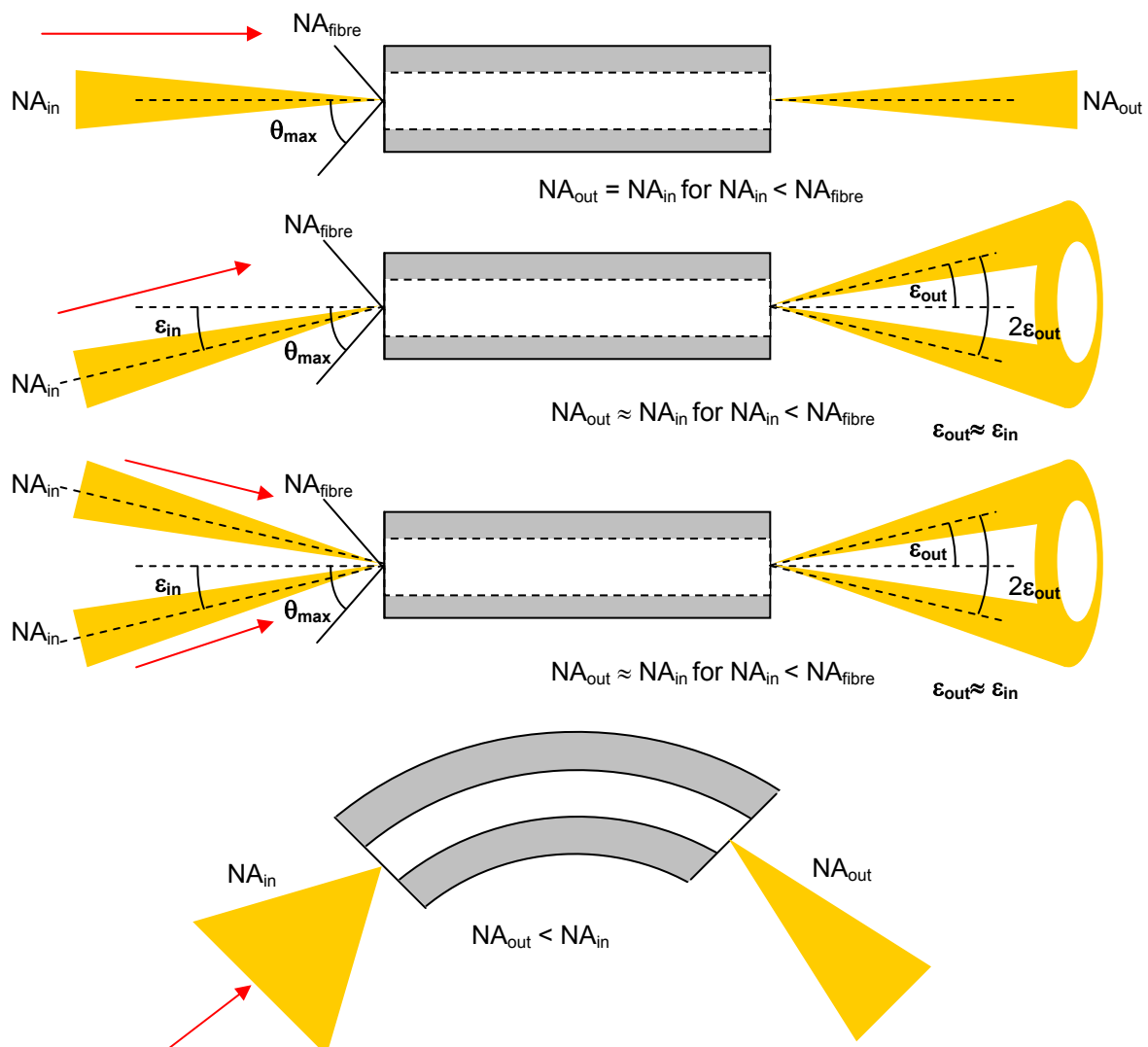
A light pulse with spectral bandwidth, $\Delta\lambda$, leads to a transit time difference Δt . As a result of the differing refractive indices between core and cladding, and their associated wavelength dependence, light in light guides travels with differing velocities. Careful material selection can limit transit time differences for specific wavelength regions.

Emitted radiation from fibres

In principle, the radiated energy of a fibre is enclosed in the fibre's aperture angle 2θ . Loss mechanisms, which reduce the number of modes in the fibre core, limit the presence of higher modes. The radiated angle is therefore smaller than the specified aperture angle. In bent cylindrical fibers, the first order approximation of the effective numerical aperture, NA^* , is:

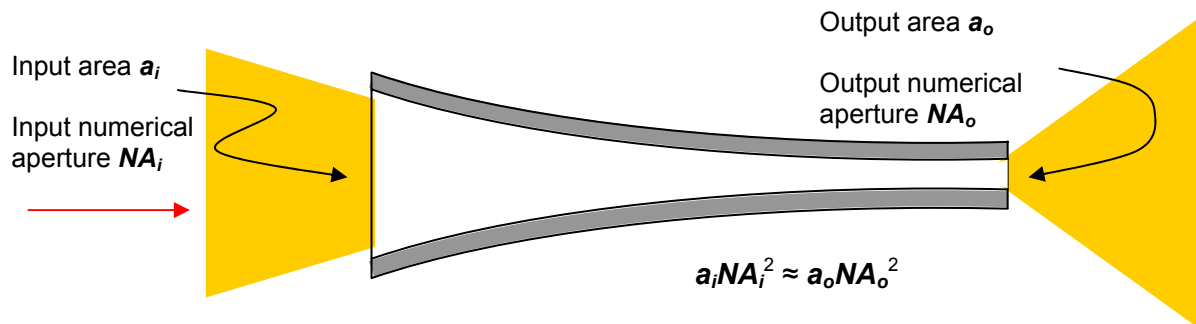
$$NA^* = \sin(\theta^*) = \sqrt{[n_1^2 - n_2^2 (1 + D_F/2R)^2]}$$

Various scattering processes in the core (Rayleigh or Mie Scattering) can convert a portion of the light power from lower modes to higher modes and therefore 'fill' the specified numerical aperture. In general the output light aperture, NA_{out} is equal to or less than that of the light coupled in the fibre, NA_{in} , provided that NA_{in} does not exceed the aperture of the fibre NA_{Fibre} . The essential characteristics associated with radiating multimode fibres are shown below.



Tapered Fibres

By tapering a single fibre, it is possible to trade off between area and solid angle. Of course the étendue (approximate product of area and solid angle) must remain constant.



Fibre Bundles

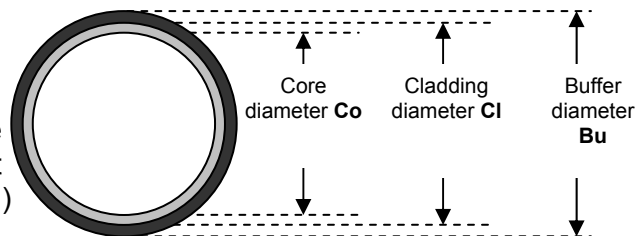
To achieve high throughput with flexible glass or quartz fibres, multiple fibres are often arranged in a bundle. This is also desirable when light sources are not point-like and thus cannot be focused to small diameters. However light losses are inevitable for two reasons:



1. For a given fibre, the maximum usable area is defined by the core and cladding diameters. These diameters determine the fibre packing factor (FPF)
2. When fibres are arranged in a bundle, not all of the bundle cross-sectional area is filled with fibres, even when tightly packed arrangements are used. The particular packing arrangement defines the bundle packing fraction (BPF)

The fibre packing factor is the ratio of useable area (core) to total surface area, as defined by the total diameter, which includes the core and cladding and buffer).

This value determines what percentage of the light striking the face of the fibre will make it into core, and thus transmitted. The FPF (in %) can be calculated from:



$$FPF = 100 C_o^2 / B_u^2$$

For example, in the case of a 100 μm diameter core and an overall diameter of 125 μm ,

$$FPF = 100 \times 100^2 / 125^2 = 64\%$$

In this example only a maximum of 64 % of the light striking the fibre has any chance of getting through, since only 64% of the end of the fibre is available for collecting light. This gets worse when the fibres are packed into bundles. The space between the individual fibres is also not transmissive, and contributes to a reduced packing fraction.

The actual number of fibres, N , of diameter d , which can be packed in a circle of diameter D , can be determined from the following relations:

$$D = (2m+1) \times d, \text{ and } N = 1 + \sum_0^m 6n$$

where m is the number of rings around the central fibre in the pack.

This is illustrated in the diagram and the table overleaf, normalised for a total fibre area of unity and where the total bundle area is A .

Bundle diameter D	Fibre number N	Number of rings m	Total bundle area A	Total fibre area	Bundle packing fraction BPF
1	1	0	1	1	100 %
3	7	1	9	7	77.78 %
5	19	2	25	19	76.00 %
7	37	3	49	37	75.51 %
9	61	4	81	61	75.31 %
11	91	5	121	91	75.21 %
13	127	6	169	127	75.15 %
15	169	7	225	169	75.11 %
17	217	8	289	217	75.09 %

More generally, for large numbers of circular fibres packed in a tight hexagonal array, the number of fibres, **N**, is given by:

$$N = 0.75 (D^2/d^2),$$

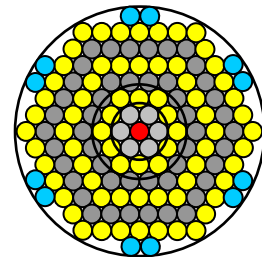
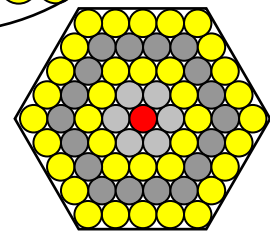
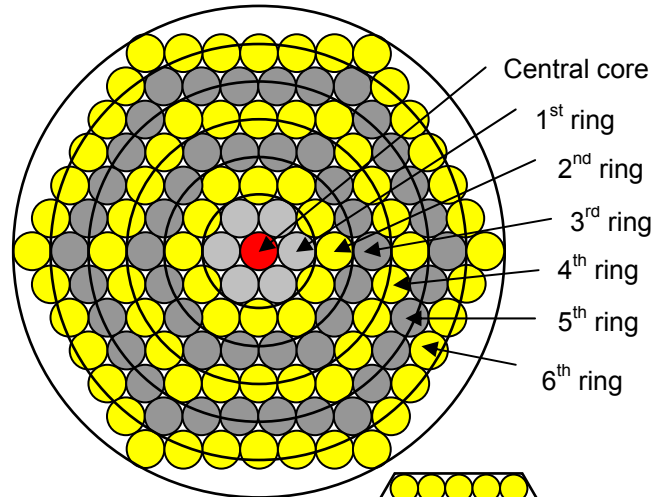
The bundle packing fraction is thus given by:

$$BPF = (N \pi d^2) / 4 A$$

Although hexagonal packing is the most efficient manner of packing circular shapes, this is only true when the external shape is hexagonal, rather than circular, as shown on the figure on the right. When the number of fibres is 7, the circular shape BPF is adequate, as shown in the table above (BPF of close to 78%). The table above refers to a circular outer shape and various approaches can be used to increase the BPF above the 75% limit suggested by the table above.

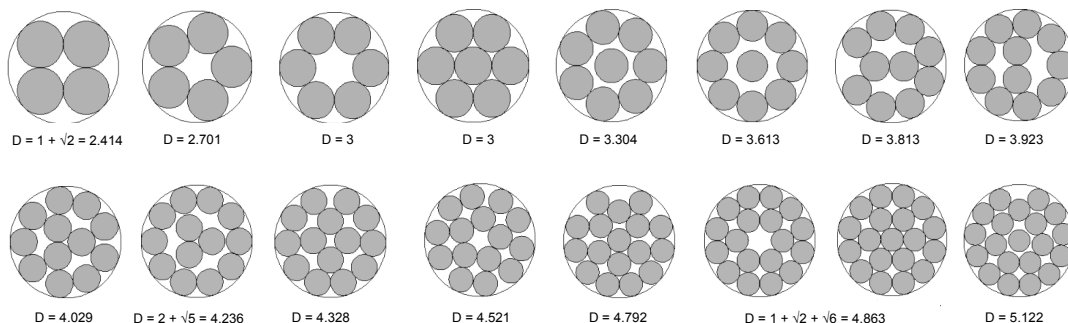
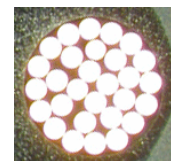
For example, by increasing the diameter very slightly (by ~1.5 %), one can do somewhat better, as shown below:

	Fibre number N	Total bundle area A	Total fibre area	Bundle packing fraction BPF
Hexagonal packing in circle	127	169	127	75.15 %
Optimised hexagonal packing in circle	139	3.2% increase to 174.24	139	79.77%



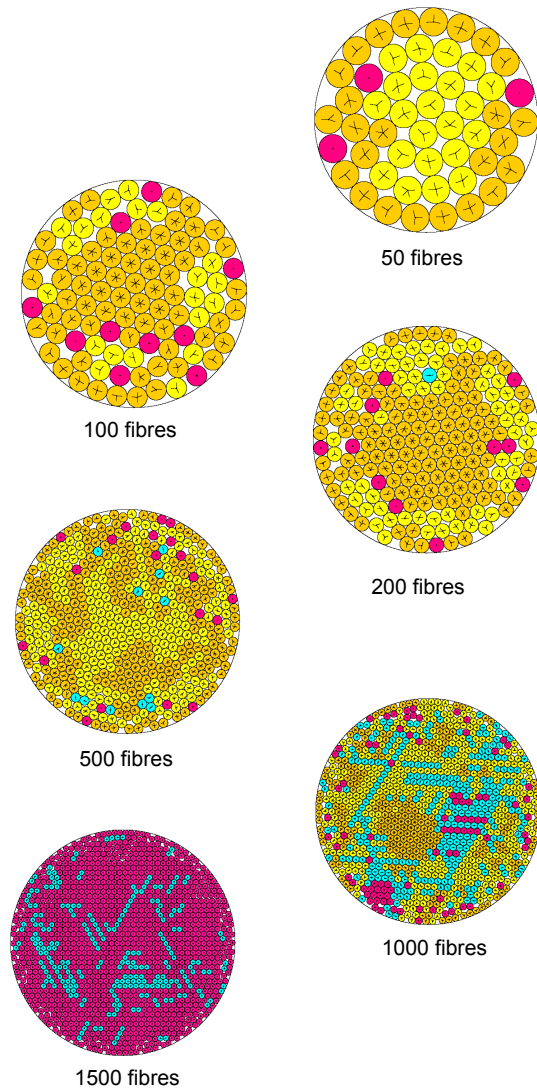
Numerous other arrangements are possible, as indicated below. However, now one enters a fairly complex branch of mathematics and in many cases, there are no known solutions.

The interested reader is referred to the excellent web sites: <http://hydra.nat.uni-magdeburg.de/packing/cci/cci.html> and <http://www2.stetson.edu/~efriedma/cirincir/> which deal with this type of problem and from which subsequent information has been borrowed.



The listing and images below show how the BPF can increase and approach 90% as the number of fibres increases. It has to be pointed out that while these numbers are optimal, they are hard to achieve in practice. Anyone who has handled more than a dozen or so fine and delicate fibres will know that fibres have, more often than not, a mind of their own. Furthermore, while it may be possible to 'fit' fibres at one end of a bundle into a ferrule, when the other end is tackled, the Russian expression 'Niet' takes over!!.

Number of fibres N	Fibre radius d	distance between fibre centres	Bundle packing fraction BPF
1	1.000		100.00%
2	0.500	2.0000	50.00%
3	0.464	1.7321	64.617%
4	0.414	1.4142	68.629%
5	0.370	1.1756	68.521%
6	0.3333	1.0000	66.667%
7	0.3333	1.0000	77.778%
8	0.30259	0.86777	73.250%
9	0.27677	0.76537	68.941%
10	0.26226	0.71098	68.780%
20	0.19522	0.485164	76.225%
30	0.161350	0.384783	78.101%
40	0.140374	0.326592	78.819%
50	0.125825	0.287873	79.160%
60	0.115657	0.261567	80.260%
70	0.107001	0.239646	80.145%
80	0.100319	0.223011	80.512%
90	0.094822	0.209510	80.921%
100	0.090235	0.1983709	81.424%
120	0.082746	0.1804205	82.162%
140	0.076563	0.1658224	82.067%
160	0.071836	0.1547923	82.567%
180	0.067829	0.1455299	82.815%
200	0.064669	0.1382813	83.643%
300	0.053153	0.1122739	84.758%
400	0.046105	0.0966671	85.027%
500	0.041437	0.0864568	85.852%
600	0.037840	0.0786553	85.910%
800	0.032872	0.0679782	86.444%
1000	0.029449	0.0606849	86.724%
1250	0.026357	0.0541405	86.835%
1500	0.024137	0.0494679	87.389%



In addition to flexibility, fibre bundles have other potential advantages in illumination systems:

- Splitting the bundle: by feeding a large fibre bundle with a single light source and splitting the bundle into two or more branches, it is possible to illuminate multiple locations, from multiple angles, with one source.
- They can be used to merge light from several sources into a single output.
- Mixed bundle: when illuminating with light over a wide spectral band, such as the full optical spectrum (e.g. ~250 nm to 2500 nm), a mixed bundle of high OH silica fibres for good UV transmission and low OH silica fibres for good IR transmission can compensate for the lack of an adequate single-fibre type.
- Shape conversion: In some situations, such as when illuminating a spectrometer, it can be useful to convert a circular cross-section of fibres to a line cross-section to align with, or actually become, the entrance slit to the spectrometer.

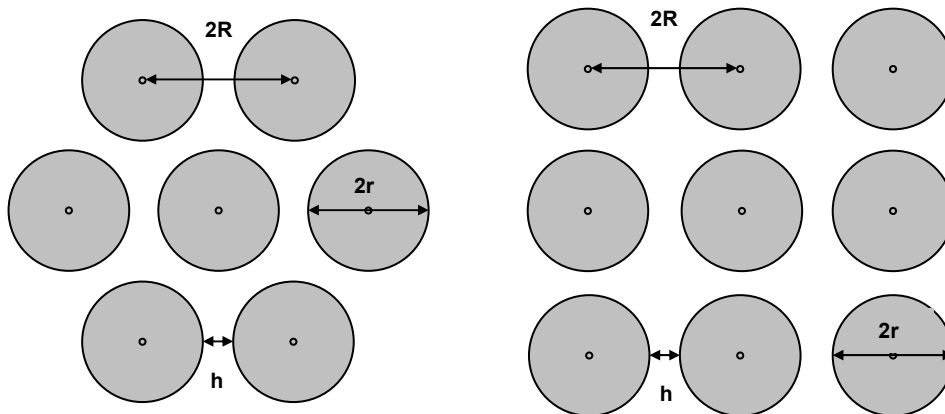
Whatever packing arrangement is used, it must be remembered that the fibre packing fraction must be included when determining the overall transmission. This is typically rarely above 80% even when the buffer has been removed from the fibre. In some cases the cladding can be made extremely thin to improve the FPF. However, the fibre then becomes even more fragile.

Furthermore, there will be the usual 4% surface reflection losses, since the fibres are rarely if ever anti-reflection coated (to the best of the authors' knowledge). For completeness, the simplified relationship of reflectivity R of an optical surface of light travelling through a medium of refractive index n_m and normally incident on a surface of refractive index n_s is:

$$R = [(n_s - n_m)/(n_s + n_m)]^2$$

It should thus be obvious that the total light transmission of fibre bundles rarely, if ever, exceeds 0.96 (surface) x 0.8 (fibres) x 0.85 (packing) x 0.96 (surface) = 0.63

The following relationships may also be found useful when dealing with buffered or clad fibres:



$$BPF = \left(\frac{\pi}{2\sqrt{3}}\right)\left(\frac{r}{R}\right)^2$$

$$BPF = \left(\frac{\pi}{4}\right)\left(\frac{r}{R}\right)^2$$

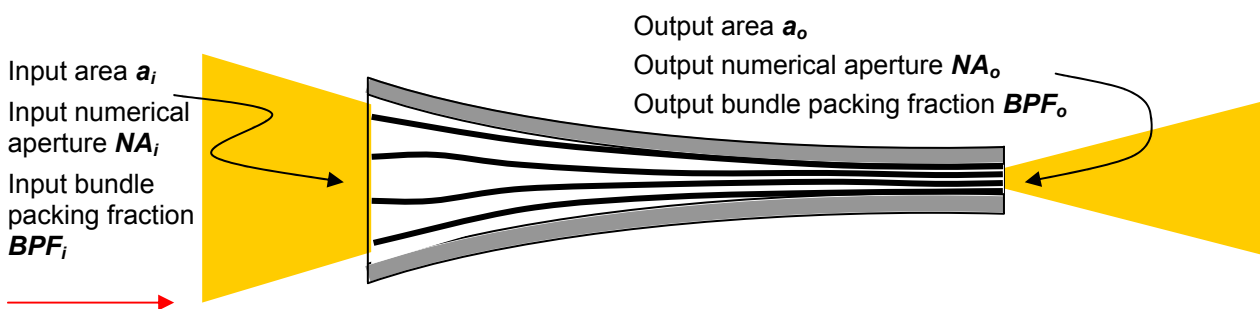
$$h = 2r \left[\left(\frac{\pi}{2 BPF \sqrt{3}} \right)^{1/2} - 1 \right]$$

$$h = 2r \left[\left(\frac{\pi}{4 BPF} \right)^{1/2} - 1 \right]$$

Very useful information on practical details of optical fibre bundle can be found at the web site of Fiberoptics Technology, Inc <http://www.fiberoptix.com/> and a useful bundle calculator can be found at: http://www.fiberoptix.com/technical/fiber_count_calculator.php.

Tapered Bundles

By tapering a fibre bundle, it is also possible to trade off between area and solid angle. Once again the étendue (approximate product of area and solid angle) must remain constant. When a bundle of straight fibres is tapered, the trade-off is between the bundle area and bundle packing fraction.



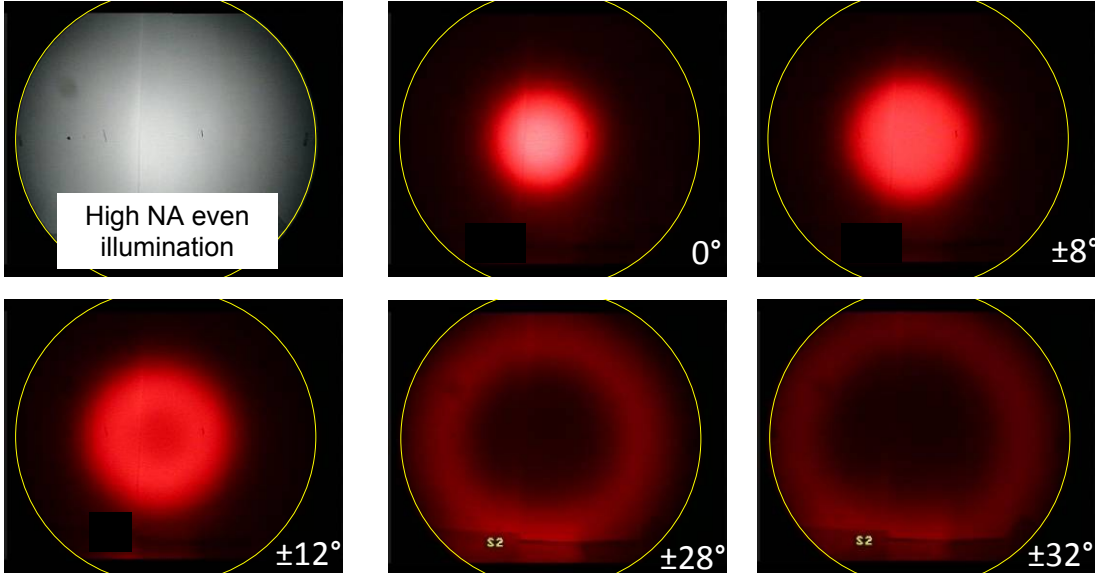
$$NA_o = NA_i = NA_{\text{fibre}}$$

$$a_o \cdot BPF_o = a_i \cdot BPF_i$$

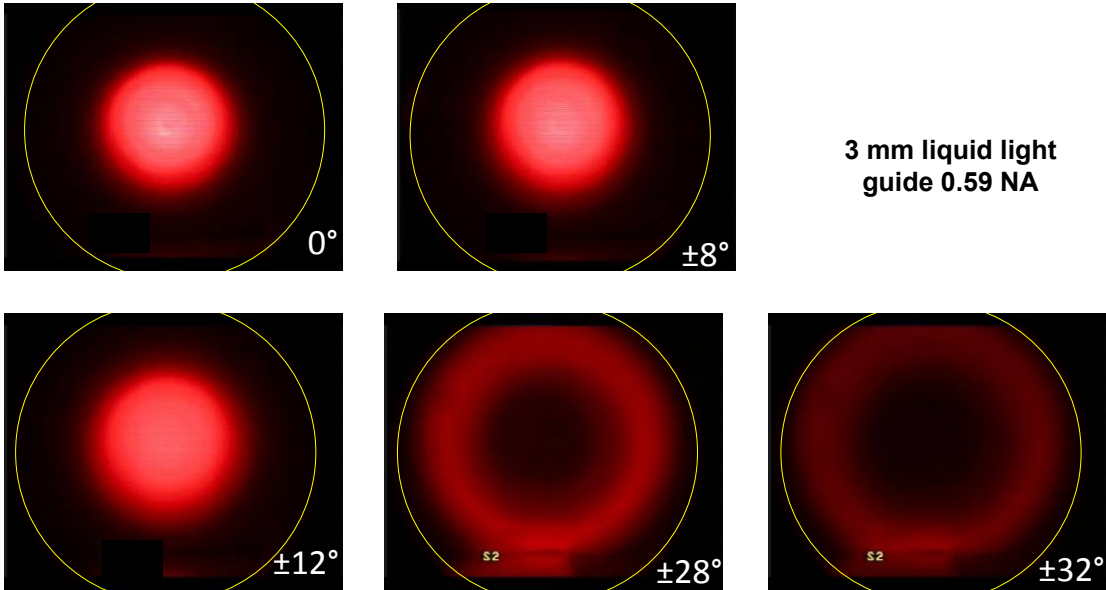
Fibre bundles 'scramble' an input light beam in much the same way as individual fibres do as described earlier. This is exemplified by measurements performed on a 5 mm diameter glass fibre bundle, as shown below. Here we compare the far-field output of this bundle when it is illuminated by an even high na illumination (top left) with far field outputs when the bundle is illuminated with a small diameter (~1.5 mm) nominally collimated laser beam at different angles of incidence to the bundle surface (other panels).

At angles $> \sim 12^\circ$, a 'hole' appears in the centre, indicating that light at low incidence angles is necessary to provide a uniform output.

5 mm fibre bundle 0.45 NA



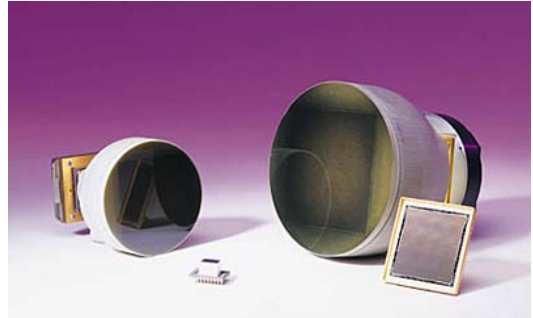
Very similar results are obtained when a single light guide is used, as shown below. Here a liquid-filled 3 mm diameter guide is used.



Imaging fibre bundles

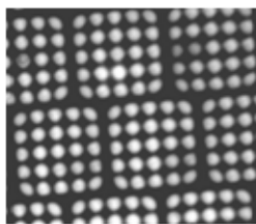
An imaging fibre bundle (also known as a coherent fibre bundle) is a collection of single optical fibres strands assembled together so that the relative orientation of the individual fibres is maintained throughout the length of the bundle. The result is that any pattern of illumination incident at the input end of the bundle is maintained and ultimately emerges from the output end. In other words, the input image is preserved. Imaging fibre bundles can be constructed in a variety of shapes and sizes, with the most common having a circular cross section. Magnification can be achieved by the use of tapered fibres in the bundle.

These bundles can be constructed in the form of solid blocks or from flexible fibres. The former are often used to bring a large image onto a sensor (e.g. a CCD imager), as shown in the image on the right (courtesy of Photometrics). In most cases, the bundle is bonded onto the imaging chip directly (i.e. bypassing the cover glass in front of the sensor), using oil (semi-permanent) or other more permanent proprietary processes. Maximum diameters of the input face can be as large as 150 mm.

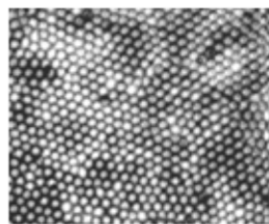


Of course, the larger the fibre bundle's magnification, the greater the reduction in effective NA. Fiber bundles with a 1:1 magnification, also known as 'stubs', provide the highest throughput. Applications requiring the highest possible light-collection efficiency benefit most by using large CCDs to reduce the amount of demagnification required.

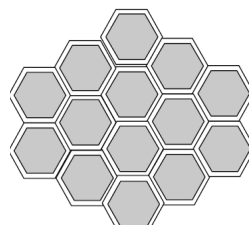
When longer image guidance is required (e.g. endoscopes) or borescopes (used for internal inspection of complex technical systems), leached fibre technology is often used. Large diameter fibres are assembled into very flexible coherent bundles, constructed by multiple draws of a high index core glass, with a lower index clad glass and an acid-soluble jacket glass. Another way to transfer images is through the use of wound flexible image components. This alternative fibre ribbon stacking method produces larger rectangular image formats. The wound stacks are then further stacked together, as shown in the figure below, The third way that coherent bundles are produced is by fusing the assembled ends, also shown below. This last process results in a somewhat higher packing density at the expense of evenness of transmission.



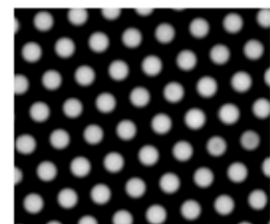
Wound bundle



Fused bundle



Fused bundle detail



Leached bundle

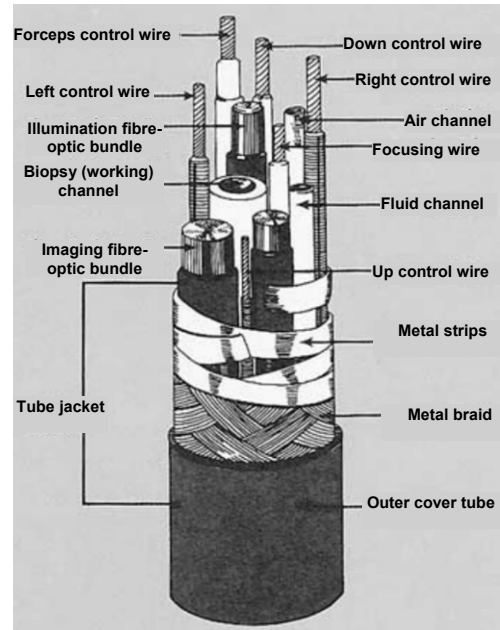
Fibres within the bundle are often $<8 \mu\text{m}$ in diameter and can be several metres long. Some intubating endoscopes may contain 30000 individual fibres in each bundle and it is currently possible to fit 50000-70000 fibres in a 1 mm diameter bundle.

Each fibre bundle is secured at either end by a binding ring then cut and polished. The mid portion of the fibres are often unbound (except to surround them in a soft plastic cover) to enable them to bend freely. On older endoscopes a small amount of a dry graphite lubricant ('Molycoat') was used to help fibres to move smoothly in relation to another when bending the within the device; on more modern endoscopes a silicone lubricant is used. An unbound fibre bundle is shown on the right.



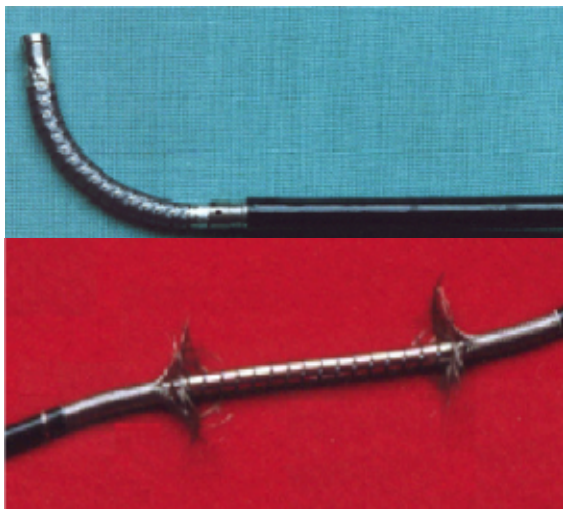
┌ 10 mm ─┐

A typical endoscope, shown below, is assembled within a 11 mm diameter insertion tube that allows excellent insertion capability (!). Such endoscopes also offer a full-size 3.2 mm working channel, a wide 110° angle of view and a tight bending radius. An objective lens is often placed at the working tip to provide non-contact focus of the observation scene.



The distal tip of the endoscope, the bending section, is capable of upward and downward angular movement. This movement is controlled by a control lever on the output section of the endoscope. In older endoscopes this lever rotated a cogwheel/chain assembly attached to control wires which run to the tip. On more modern endoscopes the control wires make one turn around a drum (the feeding mechanism) and movement is ensured due to friction between wire and drum. The control wires are sheathed with outer braided cable, in a manner similar to that used on a bicycle brake cable (Bowden cable), to resist wear and to ensure that up/down movement occurs only at the tip. The bending section is constructed using either of a series of jointed steel rings or using a kink-resistant mesh braiding. This section is designed to maintain a constant internal diameter during up/down or left-right movement and so prevent the patient tube contents being crushed. This section is then covered by a waterproof soft latex free rubber jacket.

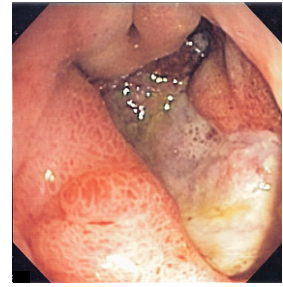
Endoscopes contain at least one channel which can be used for suction or instillation of oxygen or fluids (e.g. a local anaesthetic or saline solution). Bronchosopes carry the largest channels which are most effective for removing secretions or tissues (e.g. biopsies). The suction channel in the smallest 'scopes, such as those intended for paediatric use, is omitted.



The patient tube protects the fibre bundles and the tip control mechanism. The patient tube is made to be flexible and crush resistant, able to resist deformation resulting from rotational forces (torque control of the tip). These requirements are satisfied by constructing the patient tube out of three layers. The first layer is a continuous stainless steel coil from the proximal end of the bending section to the fibrescope body. The second layer is a tough stainless steel mesh braid. Finally an outer, fluid resistant layer is applied. The bundle carrying fibres from the light source is constructed in the same way as the patient tube.

All in all, a really neat piece of engineering, even

though the images thus produced are sometimes of limited quality, due to the inevitably low number of fibres in the bundle. Nevertheless, they are adequate for numerous diagnostic procedures. An example of a deep gastric ulcer as seen with a bundle endoscope is shown on the right.



Continuing with the high-tech theme, light guide bundle can also be used to perform endo-microscopy (contact imaging) or confocal fluorescence endomicroscopy. In the latter case, a laser beam scans the output side of the bundle, is transferred to the input side, where it excites fluorescence. The fluorescence emission returns down the bundle, where it is descanned and detected. Significant image processing is used (sometimes delivering artefacts) to obtain diffraction-limited images. Mauna Kea Technologies is the leading company, at the time of writing, which provides such instrumentation, although it is possible to develop similar systems in the laboratory.

This note was prepared in December 2012 by B. Vojnovic, with help from D Volpi.

The financial support of Cancer Research UK, the MRC and EPSRC is gratefully acknowledged.

© Gray Institute, Department of Oncology, University of Oxford, 2012.

This work is licensed under the Creative Commons Attribution-NonCommercial-NoDerivs 3.0 Unported License. To view a copy of this license, visit <http://creativecommons.org/licenses/by-nc-nd/3.0/> or send a letter to Creative Commons, 444 Castro Street, Suite 900, Mountain View, California, 94041, USA.